

LETTER • OPEN ACCESS

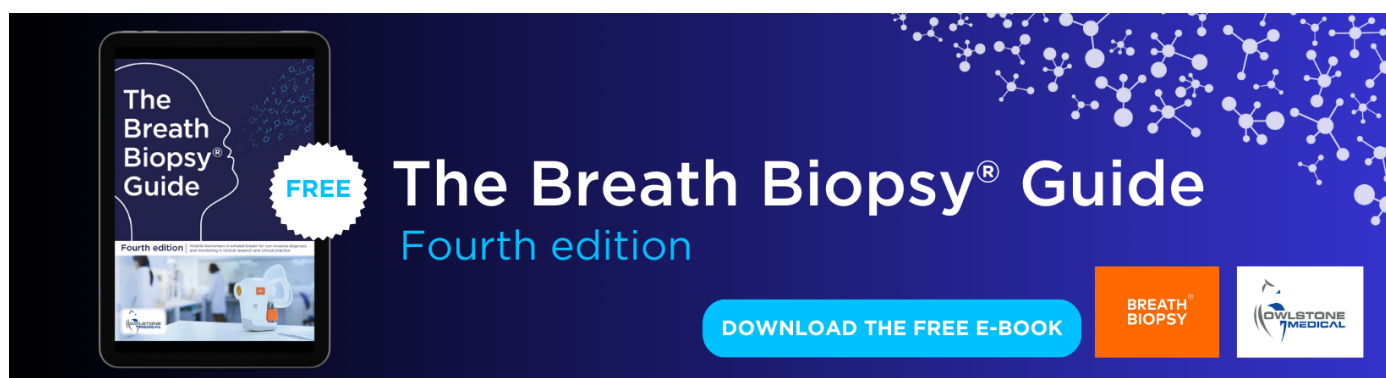
The biophysical climate mitigation potential of boreal peatlands during the growing season

To cite this article: Manuel Helbig *et al* 2020 *Environ. Res. Lett.* **15** 104004

View the [article online](#) for updates and enhancements.

You may also like

- [Forestland-peatland hydrologic connectivity in water-limited environments: hydraulic gradients often oppose topography](#)
K J Hokanson, E S Peterson, K J Devito et al.
- [The influence of system heterogeneity on peat-surface temperature dynamics](#)
R Leonard, P Moore, S Krause et al.
- [Drainage canal impacts on smoke aerosol emissions for Indonesian peatland and non-peatland fires](#)
Xiaoman Lu, Xiaoyang Zhang, Fangjun Li et al.



The Breath Biopsy® Guide
Fourth edition

DOWNLOAD THE FREE E-BOOK

BREATH BIOPSY

OWLSTONE MEDICAL

Environmental Research Letters



LETTER

OPEN ACCESS

RECEIVED

24 April 2020

REVISED

24 July 2020

ACCEPTED FOR PUBLICATION

31 July 2020

PUBLISHED

15 October 2020

Original content from this work may be used under the terms of the [Creative Commons Attribution 4.0 licence](#).

Any further distribution of this work must maintain attribution to the author(s) and the title of the work, journal citation and DOI.



The biophysical climate mitigation potential of boreal peatlands during the growing season

Manuel Helbig^{1,2} , James M Waddington¹ , Pavel Alekseychik^{3,4} , Brian Amiro⁵ , Mika Aurela⁶ , Alan G Barr^{7,8} , T Andrew Black⁹ , Sean K Carey¹ , Jiquan Chen¹⁰ , Jinshu Chi¹¹ , Ankur R Desai¹² , Allison Dunn¹³ , Eugenie S Euskirchen¹⁴ , Lawrence B Flanagan¹⁵ , Thomas Friborg¹⁶ , Michelle Garneau¹⁷ , Achim Grelle¹⁸ , Silvie Harder¹⁹ , Michal Heliasz²⁰ , Elyn R Humphreys²¹ , Hiroki Ikawa²² , Pierre-Erik Isabelle²³ , Hiroki Iwata²⁴ , Rachhpal Jassal⁹ , Mika Korkiakoski⁶ , Juliya Kurbatova²⁵ , Lars Kutzbach²⁶ , Elena Lapshina²⁷ , Anders Lindroth²⁸ , Mikael Ottosson Löfvenius¹¹ , Annalea Lohila^{3,6} , Ivan Mammarella³ , Philip Marsh²⁹ , Paul A Moore¹ , Trofim Maximov³⁰ , Daniel F Nadeau²³ , Erin M Nicholls¹ , Mats B Nilsson¹¹ , Takeshi Ohta³¹ , Matthias Peichl¹¹ , Richard M Petrone³² , Anatoly Prokushkin³³ , William L Quinton²⁹ , Nigel Roulet¹⁹ , Benjamin R K Runkle^{26,34} , Oliver Sonnentag³⁵ , Ian B Strachan³⁶ , Pierre Taillardat¹⁷ , Eeva-Stiina Tuittila³⁷ , Juha-Pekka Tuovinen⁶ , Jessica Turner¹² , Masahito Ueyama³⁸ , Andrej Varlagin²⁵ , Timo Vesala³⁹ , Martin Wilmking⁴⁰ , Vyacheslav Zyrianov³³ and Christopher Schulze⁴¹

¹ School of Earth, Environment and Society, McMaster University, Hamilton, ON, Canada

² Department of Physics and Atmospheric Science, Dalhousie University, Halifax, NS, Canada

³ Institute for Atmospheric and Earth System Research/Physics, Faculty of Sciences, University of Helsinki, Helsinki, Finland

⁴ Natural Resources Institute Finland (LUKE), Bioeconomy and Environment, Helsinki, Finland

⁵ Department of Soil Science, University of Manitoba, Winnipeg, MB, Canada

⁶ Finnish Meteorological Institute, Helsinki, Finland

⁷ Climate Research Division, Environment and Climate Change Canada, Saskatoon, SK, Canada

⁸ Global Institute for Water Security, University of Saskatchewan, Saskatoon, SK, Canada

⁸ Faculty of Land and Food Systems, The University of British Columbia, Vancouver, BC, Canada

¹⁰ Department of Geography, Environment, and Spatial Sciences, Michigan State University, MI, United States of America

¹¹ Department of Forest Ecology and Management, Swedish University of Agricultural Sciences, Umea, Sweden

¹² Department of Atmospheric Sciences and Oceanic Sciences, University of Wisconsin-Madison, Madison, WI, United States of America

¹³ Department of Earth, Environment, and Physics, Worcester State University, Worcester, MA, United States of America

¹⁴ Institute of Arctic Biology, University of Alaska Fairbanks, Fairbanks, AK, United States of America

¹⁵ Department of Biological Sciences, University of Lethbridge, Lethbridge, AB, Canada

¹⁶ Department of Geosciences and Natural Resource Management, University of Copenhagen, Copenhagen, Denmark

¹⁷ Université du Québec à Montréal - Geotop, Montréal, QC, Canada

¹⁸ Department of Ecology, Swedish University of Agricultural Sciences, Uppsala, Sweden

¹⁹ Department of Geography, McGill University, Montréal, QC, Canada

²⁰ Centre for Environmental and Climate Research, Lund University, Lund, Sweden

²¹ Department of Geography and Environmental Studies, Carleton University, Ottawa, ON, Canada

²² Institute for Agro-Environmental Sciences, National Agriculture and Food Research Organization, Tsukuba, Japan

²³ Département de génie civil et de génie des eaux, Université Laval, Quebec City, QC, Canada

²⁴ Department of Environmental Science, Faculty of Science, Shinshu University, Matsumoto, Japan

²⁵ A.N. Severtsov Institute of Ecology and Evolution, Russian Academy of Sciences, Russia

²⁶ Institute of Soil Science, University of Hamburg, Hamburg, Germany

²⁷ Center of Environmental Dynamics and Climate Changes, Yugra State University, Khanty-Mansiysk, Russia

²⁸ Department of Physical Geography and Ecosystem Science, Lund University, Lund, Sweden

²⁹ Cold Regions Research Centre, Wilfrid Laurier University, Waterloo, ON, Canada

³⁰ Institute for Biological Problems of Cryolithosphere, Siberian Branch Russian Academy of Sciences, Yakutsk, Russia

³¹ Graduate School of Bioagricultural Sciences, Nagoya University, Nagoya, Japan

³² Department of Geography and Environmental Management, University of Waterloo, Waterloo, ON, Canada

³³ V.N. Sukachev Institute of Forest, Siberian Branch of the Russian Academy of Sciences, Krasnoyarsk, Russia

³⁴ Department of Biological & Agricultural Engineering, University of Arkansas, Fayetteville, AR, United States of America

³⁵ Département de géographie & Centre d'études nordiques, Université de Montréal, Montréal, QC, Canada

³⁶ Department of Natural Resource Sciences, McGill University, Sainte-Anne-de-Bellevue, QC, Canada

³⁷ School of Forest Sciences, University of Eastern Finland, Joensuu, Finland

³⁸ Graduate School of Life and Environmental Sciences, Osaka Prefecture University, Sakai, Japan

³⁹ Institute for Atmospheric and Earth System Research/Forest Sciences, Faculty of Agriculture and Forestry, University of Helsinki, Finland

⁴⁰ Institute of Botany and Landscape Ecology, University of Greifswald, Greifswald, Germany

⁴¹ Department of Renewable Resources, University of Alberta, Edmonton, Alberta, Canada

E-mail: manuel.helbig@dal.ca

Keywords: peatlands, boreal forest, climate mitigation, regional climate, energy balance

Supplementary material for this article is available [online](#)

Abstract

Peatlands and forests cover large areas of the boreal biome and are critical for global climate regulation. They also regulate regional climate through heat and water vapour exchange with the atmosphere. Understanding how land-atmosphere interactions in peatlands differ from forests may therefore be crucial for modelling boreal climate system dynamics and for assessing climate benefits of peatland conservation and restoration. To assess the biophysical impacts of peatlands and forests on peak growing season air temperature and humidity, we analysed surface energy fluxes and albedo from 35 peatlands and 37 evergreen needleleaf forests—the dominant boreal forest type—and simulated air temperature and vapour pressure deficit (VPD) over hypothetical homogeneous peatland and forest landscapes. We ran an evapotranspiration model using land surface parameters derived from energy flux observations and coupled an analytical solution for the surface energy balance to an atmospheric boundary layer (ABL) model. We found that peatlands, compared to forests, are characterized by higher growing season albedo, lower aerodynamic conductance, and higher surface conductance for an equivalent VPD. This combination of peatland surface properties results in a $\sim 20\%$ decrease in afternoon ABL height, a cooling (from 1.7 to 2.5 °C) in afternoon air temperatures, and a decrease in afternoon VPD (from 0.4 to 0.7 kPa) for peatland landscapes compared to forest landscapes. These biophysical climate impacts of peatlands are most pronounced at lower latitudes ($\sim 45^\circ\text{N}$) and decrease toward the northern limit of the boreal biome ($\sim 70^\circ\text{N}$). Thus, boreal peatlands have the potential to mitigate the effect of regional climate warming during the growing season. The biophysical climate mitigation potential of peatlands needs to be accounted for when projecting the future climate of the boreal biome, when assessing the climate benefits of conserving pristine boreal peatlands, and when restoring peatlands that have experienced peatland drainage and mining.

1. Introduction

Peatlands are found throughout the boreal biome and cover about 15% of the boreal land area (Xu *et al* 2018). In some boreal regions such as the Hudson Bay Lowlands and the Western Siberian Lowlands, peatlands cover close to 100% of the land surface (figure 1). Nevertheless, current Earth system models do not specifically account for peatlands as a plant functional type and simulate the boreal biome as a forest ecosystem (e.g. Poulter *et al* 2011). The lack of peatlands in global climate simulations could therefore lead to biases in regional climate projections for the boreal biome (Helbig *et al* 2020).

Peatlands north of 45°N store about 500 Gt of belowground carbon (Loisel *et al* 2014), which is about half of the carbon currently stored in the atmosphere (Friedlingstein *et al* 2019). With over 300 000 km² of boreal and temperate peatlands ($\sim 10\%$ of total boreal and temperate peatland area) having been mined or drained for agriculture and forestry (Xu *et al* 2018, Günther *et al* 2020), the loss of pristine peatlands (Chapman *et al* 2003, Turunen 2008, Rooney *et al* 2012) is not being balanced by the restoration of degraded peatlands (Chimner *et al* 2017). The drained peatland area in the boreal

zone amounts to only about 40% of the drained peatland area in the temperate zone (Günther *et al* 2020) with vast areas of boreal peatlands still being intact. Draining intact peatlands likely has implications for the global climate (Leifeld and Menichetti 2018) as peatlands exert a biogeochemical cooling effect through their long-term sequestration of carbon dioxide (Frolking and Roulet 2007) while the drainage of peatlands leads to emissions of century to millennial old carbon. In addition, biophysical land surface properties of peatlands related to the reflection of solar radiation (i.e. albedo), the transport of heat between land and atmosphere (i.e. aerodynamic conductance), and the ability of the land surface to transfer water vapor to the atmosphere (i.e. surface conductance) have the potential to alter local to regional climates through their impacts on the land surface energy balance (Helbig *et al* 2016b, Hemes *et al* 2018, Alekseychik *et al* 2018, Worrall *et al* 2019). Peatlands are usually characterised by high evapotranspiration rates during the growing season if the water table depth remains close to the surface (Lafleur *et al* 2005), i.e. partitioning more available energy into latent heat (i.e. water vapor) than into sensible heat (Lafleur 2008). In contrast, boreal needleleaf forests usually partition more available energy into

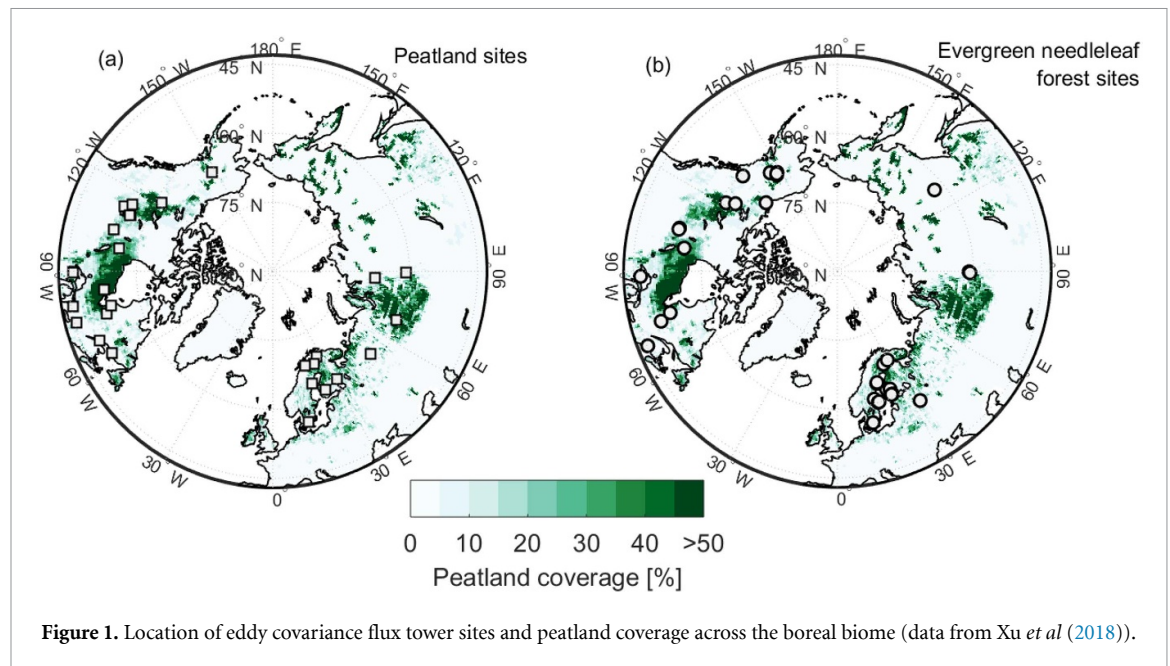


Figure 1. Location of eddy covariance flux tower sites and peatland coverage across the boreal biome (data from Xu *et al* (2018)).

sensible heat than into latent heat (Baldocchi *et al* 2000). However, long-term lowering of the water table (e.g. through drainage) in peatlands has been shown to result in a reduction of evapotranspiration and an increase in the partitioning of available energy to latent heat (Moore *et al* 2013). Using a pan-boreal evapotranspiration dataset, Helbig *et al* (2020) have shown that growing season evapotranspiration in boreal peatlands is higher than in boreal forests mainly due to higher surface conductance of peatlands. How such differences in land surface properties and surface energy fluxes may alter regional climates in the boreal biome remains uncertain. As such, to assess the net climate mitigation potential of peatlands, both the biogeochemical and biophysical impacts need to be considered since biophysical climate impacts can either amplify or attenuate the magnitude of climate warming regionally (Pielke *et al* 2002).

Studies on biophysical climate impacts in the boreal biome have commonly focussed on albedo forcing during the snow cover period (e.g. Betts 2000, Anderson *et al* 2011). However, growing season climate is particularly relevant when assessing ecological impacts of climate change caused by heat and drought stress (e.g. Way *et al* 2013). Vegetation productivity and evapotranspiration (ET, i.e. sum of evaporation and plant transpiration) is largest during the growing season with air temperature (e.g. Mäkelä *et al* 2006) and atmospheric water demand (e.g. Novick *et al* 2016) partly regulating plant productivity. During the growing season, drought stress associated with high vapour pressure deficit (VPD) can lead to increased tree mortality and in some cases to vegetation shifts (e.g. Will *et al* 2013, Trugman *et al* 2018). In a warming climate, biophysical impacts of vegetation on local to regional climate may have the potential to create

refugia for animals and plants, which are not adapted to heat and drought stress (Ackerly *et al* 2010, De Frenne *et al* 2013).

Here, we address the question whether peatland-specific biophysical land surface properties have the potential to mitigate climate warming regionally by creating cooler (i.e. lower air temperature) and more humid (i.e. lower VPD) growing season climates compared to boreal forests. We analysed sensible and latent heat flux observations from boreal peatlands and forests made with the eddy covariance (EC) technique at 72 sites and surface albedo measurements obtained from satellite-based remote sensing across the boreal biome to derive land surface characteristics for both ecosystem types. Then, we used a coupled surface-atmosphere modelling experiment to quantify the potential impact of peatlands on peak growing season air temperature and VPD.

2. Methods

2.1. Study sites

In this study, we used multi-year clear-sky peak growing season sensible and latent heat flux data and ancillary meteorological observations from 72 EC flux tower sites across the boreal biome as delineated by Olson *et al* (2001) (figure 1). The sites comprised of 35 peatlands (154 site years) that were not subject to anthropogenic disturbance and 37 managed and pristine evergreen needleleaf forest sites (239 site years). Forest sites have not been impacted by wildfire or insect disturbances or by clear-cutting for at least 30 years prior to the beginning of flux measurements. Percent tree cover (from the Moderate Resolution Imaging Spectroradiometer [MODIS] Vegetation Continuous Fields tree cover MOD44B

product, 2000–2018) was about 50% lower in peatlands ($21\% \pm 14\%$) than in forests ($57\% \pm 14\%$). The median latitudinal location of all peatland and forest sites was $56^\circ\text{N} \pm 7^\circ$ and $61^\circ\text{N} \pm 6^\circ$, respectively, and was not significantly different (Wilcoxon rank sum test, $p = 0.18$). Evergreen needleleaf forests represent the most prevalent boreal forest type in North America (Gauthier *et al* 2015) and in northern Europe (Esseen *et al* 1997). Only observations for the month of July, which coincides with peak ET rates at most boreal sites (see Helbig *et al* 2020), were used for the coupled surface-atmosphere modelling experiment. Further details about the sites can be found in Tab. S1 and in Helbig *et al* (2020).

2.2. Derivation of surface properties

The exchanges of sensible heat and water vapour between land surface and atmosphere are controlled by atmospheric forcing (e.g. radiation, VPD) and by land surface characteristics (e.g. albedo, aerodynamic and surface conductance). Here, we derived and compared three biophysical land surface properties from remote sensing observations and from EC measurements for peatland and forest ecosystems: (1) albedo (α) determines how much incoming short-wave radiation is reflected back by the land surface and thus partly controls available energy (e.g. Bonan 2008), (2) aerodynamic conductance (g_a , m s^{-1}) controls the transport of sensible and latent heat into the atmosphere (e.g. Raupach 1995), and (3) surface conductance (including canopy and soil conductance; g_s , m s^{-1}) regulates the transport of water vapour from the land surface (i.e. through stomata, moss surfaces, or soil) to the atmosphere (e.g. Schulze *et al* 1995).

2.2.1. Albedo

Mean July (white-sky) albedo (2000–2018, approximately 10:30 local time) was taken for all flux tower sites from the MODIS MCD43A3 Version 6 Albedo Model dataset (Schaaf and Wang 2015) since observations of incoming and outgoing shortwave radiation were not available for all sites. The spatial and temporal resolution of MCD43A3 is 500 m and daily, respectively. Pixels covering the flux tower locations were selected using the MODIS/VIIRS Global Subset Tool (<https://modis.ornl.gov/cgi-bin/MODIS/global/subset.pl>).

2.2.2. Aerodynamic and surface conductance

Aerodynamic and surface conductance for peatlands and forests were derived from half-hourly EC flux data. Aerodynamic conductance was calculated using friction velocity (u^* , m s^{-1}) and horizontal wind speed (U , m s^{-1}) measurements based on work by Verma (1989):

$$g_a = \left(\frac{kB^{-1}}{ku_*} \left(\frac{d_h}{d_v} \right)^{2/3} + \frac{U}{u_*^2} \right)^{-1} \quad (1)$$

where $k = 0.4$ is the von Karman's constant, d_h is the thermal diffusivity and d_v is the molecular diffusivity of water vapour and d_h/d_v is 0.89 at 20°C . In this study, we assume the excess resistance parameter $kB^{-1} = 2$ as in Humphreys *et al* (2006) and in Baldocchi and Ma (2013). Surface conductance was calculated by inverting the Penman-Monteith equation (Monteith 1965; see Helbig *et al* 2020 for more details).

$$\frac{1}{g_s} = \left(\frac{s}{\gamma} \left(\frac{R_a}{\lambda ET} - 1 \right) - 1 \right) g_a^{-1} + \frac{\rho C_p VPD}{\gamma \lambda ET}. \quad (2)$$

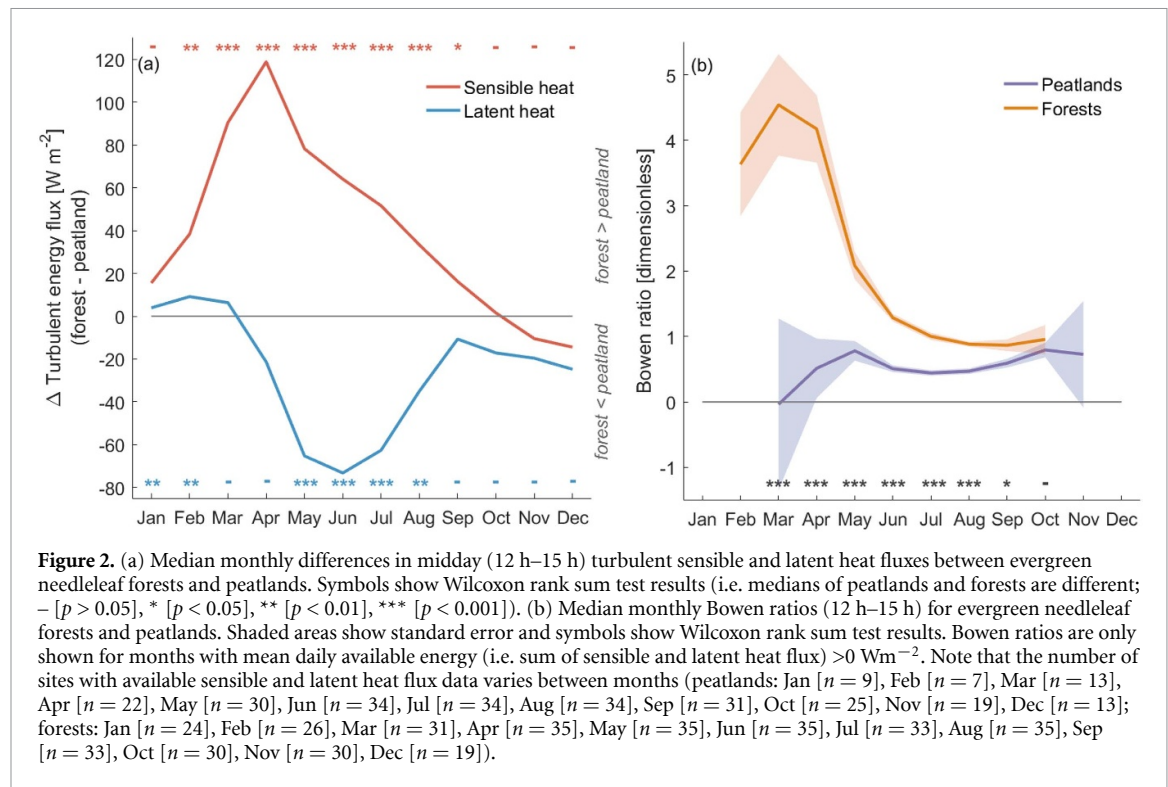
In equation (2), γ is the psychrometric constant (Pa K^{-1}), s is the slope of the saturation vapour pressure-temperature curve (Pa K^{-1}), λ is the latent heat of vaporization (J kg^{-1}), ET is evapotranspiration ($\text{kg m}^{-2} \text{s}^{-1}$), λET is the observed latent heat flux (W m^{-2}), R_a is available energy flux (W m^{-2} , here the sum of observed sensible and latent heat fluxes), ρ is air density (kg m^{-3}), and C_p is the specific heat of air at constant pressure ($\text{J kg}^{-1} \text{K}^{-1}$).

2.3. Coupled surface energy balance-atmospheric boundary layer modelling

To quantify the potential biophysical impact of peatland- and forest-specific land-atmosphere interactions on growing season climate (here approximated as July climate), we applied a coupled clear-sky surface energy balance-atmospheric boundary layer (ABL) model (e.g. van Heerwaarden *et al* 2009, Baldocchi and Ma 2013). In other studies (e.g. Baldocchi and Ma 2013, Zhang *et al* 2020, Novick and Katul 2020), paired-tower measurements were used to directly quantify land use impacts on land surface or air temperatures. This approach could not be used here since measurements over co-located peatlands and forests are generally not available. Instead, we set up two modelling experiments simulating the diurnal development of mid-growing season air temperature (T_a) and VPD over a hypothetical homogeneous peatland and a hypothetical homogeneous forest landscape. Previous studies have used a similar approach by replacing boreal forests with bare ground or bare ground in the Arctic with deciduous forest in global circulation models to assess land cover impacts on climate (Bonan *et al* 1992, Swann *et al* 2010). Latent heat exchange was calculated using the Penman-Monteith equation:

$$\lambda ET = \frac{s(R_n - G) + \rho C_p g_a VPD}{s + \gamma \left(1 + \frac{g_a}{g_s} \right)} \quad (3)$$

where R_n is net radiation (W m^{-2}) and G is soil heat flux (W m^{-2}). Soil heat flux for peatlands and forests during clear-sky days was estimated using median measured G in July during clear-sky days from 18 peatland and 16 forest sites, where such observations were available. Clear-sky days were defined



as days when measured incoming shortwave radiation (SW_{in}) steadily increased ($>75\%$ of half hours) during the eight hours before solar noon, steadily decreased during the eight hours after solar noon, and daily maximum SW_{in} was larger than 90% of the site's maximum SW_{in} in July. We identified in total 1117 and 1595 clear-sky days for July across all peatland and forest sites, respectively.

Net radiation was calculated as follows:

$$R_n = (1 - \alpha) SW_{in} + LW_{in} - LW_{out} \quad (4)$$

where LW_{in} is incoming longwave radiation (W m^{-2}), which was calculated using the Stefan-Boltzmann equation with T_a (K) and a clear-sky emissivity as described in Brutsaert (1975). Outgoing longwave radiation (LW_{out} , W m^{-2}) was calculated using the Stefan-Boltzmann equation with surface temperature (T_s , K) and an emissivity of 0.98. Incoming shortwave radiation was calculated based on latitude and day of year (Allen *et al* 2005). The surface temperature was estimated by applying a solution to the quadratic equation, which defines the difference between T_s and T_a as described in detail by Baldocchi and Ma (2013) following Paw (1987).

Sensible heat flux was then calculated as follows:

$$H = R_n - G - \lambda ET \quad (5)$$

where λET was calculated using equation (3). Mean clear-sky diurnal cycles of g_a for peatlands and forests were used to compute λET . Surface conductance was estimated using a multiple-constraint function (Schulze *et al* 1994) derived from mean

g_s responses to VPD and SW_{in} across all peatland and forest sites (see figure S1 available online at stacks.iop.org/ERL/15/104004/mmedia):

$$g_s = g_{smax} \times f(VPD) \times f(SW_{in}) \quad (6)$$

where $f(VPD)$ is a nonlinear function accounting for limitations imposed by atmospheric water demand (figure S2, with g_0 and g_1 being best-fit parameters, g_{smax} being the 97.5th percentile of g_s observed at $VPD > 0.5$, and g_{s-up} being the upper boundary of g_s ; see also Helbig *et al* 2020) given by

$$f(VPD) = \frac{g_{s-up}}{g_{smax}} = g_0 + \left(1 + \frac{g_1}{\sqrt{VPD}}\right) \quad (7)$$

and where $f(SW_{in})$ is a rectangular hyperbola function accounting for constraints imposed by light (figure S3, with b_1 and b_2 being best-fit parameters) given by

$$f(SW_{in}) = \frac{g_{s-up}}{g_{smax}} = \frac{b_1 \times b_2 \times SW_{in}}{b_1 + b_2 \times SW_{in}} \quad (8)$$

Parameters g_0 , g_1 , b_1 , and b_2 were derived by fitting $f(VPD)$ and $f(SW_{in})$ to the upper boundary line g_{s-up}/g_{smax} (Jarvis 1976, see Helbig *et al* (2020) for more details). We did not include a soil moisture function as a constraint since comparable soil moisture data across the flux tower sites were not available. Our analysis therefore focuses on differences in land-atmosphere interactions under the assumption of optimal site-specific water supply (Helbig *et al* 2020).

The growth of the ABL due to the entrainment of warm and dry air from above the top of the

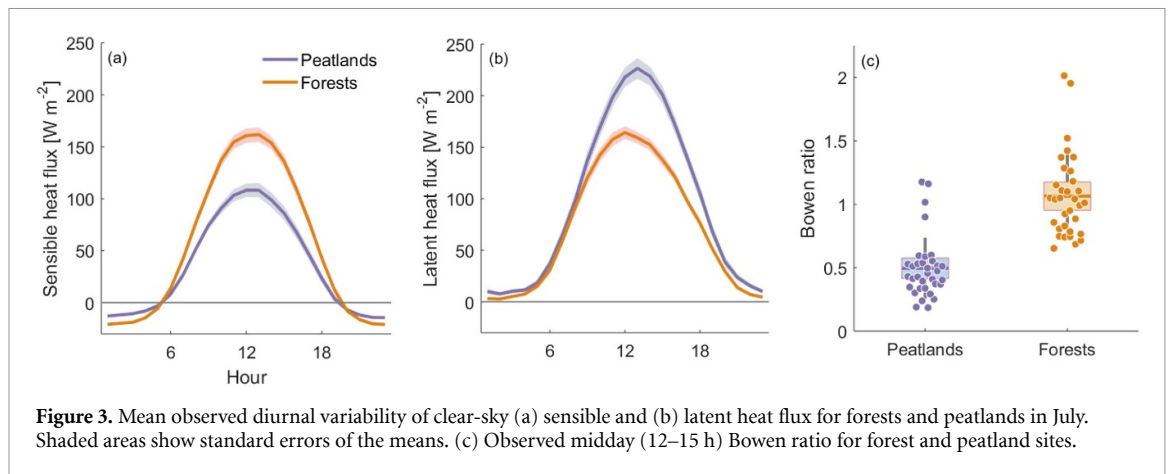


Figure 3. Mean observed diurnal variability of clear-sky (a) sensible and (b) latent heat flux for forests and peatlands in July. Shaded areas show standard errors of the means. (c) Observed midday (12–15 h) Bowen ratio for forest and peatland sites.

ABL (i.e. capping inversion) and the input of sensible heat and water vapour from the land surface determines the diurnal development of T_a and VPD (van Heerwaarden *et al* 2009). Here, we used an ABL slab growth model to quantify the impact of land-atmosphere interactions on T_a and VPD in the ABL using mean land surface parameters (α , g_a , and g_s) specific to peatland and forest ecosystems. Such models assume temperature and specific humidity in the ABL to be well-mixed and have been used to assess how land use and cover (e.g. Bagley *et al* 2011, Baldocchi and Ma 2013) and plant responses to water stress (e.g. Combe *et al* 2016) influence the mean ABL state variables T_a , VPD, and ABL height. We used an ABL slab model as implemented in the Chemistry Land-surface Atmosphere Soil Slab model (CLASS, van Heerwaarden *et al* 2010, Vila-guerau de Arellano *et al* 2015, Wouters *et al* 2019). The ABL slab model was run for clear-sky conditions to simulate diurnal daytime development of T_a and VPD between 05 h and 19 h local time for July. In our modelling experiment, we assumed that the ABL is underlain by a homogeneous peatland or by a homogeneous forest landscape. It should therefore be noted that the climate impacts reported here likely represent the upper end of such effects since forests and peatlands mostly occur as a mosaic in the boreal biome.

Initial mixed-layer potential temperature (T_p) and specific humidity (q) (at 05 h local time) and T_p and q lapse rates in the free atmosphere above the ABL are required to parameterize the ABL model. The initial atmospheric conditions and lapse rates were kept the same for the peatland and forest model runs and were taken from eight atmospheric balloon sounding sites across a latitudinal gradient in Canada and the U.S. ranging from 46° N to 68° N (Tab. S2). Balloon sounding data was accessed through the Department of Atmospheric Science website at the University of Wyoming (<http://weather.uwyo.edu/upperair/sounding.html>). To derive initial T_p and q and their free-atmosphere lapse rates, we used balloon sounding data for July (2008–2017). Initial T_p and q were taken as the lowest

level (100 m to 400 m above ground) of morning atmospheric profiles of T_p and q (collected at 12 h Coordinated Universal Time, i.e. 04 h–08 h local time at the study sites). Lapse rates in the free atmosphere were estimated as the slope parameter of linear regressions of height on T_p and on q (from morning profiles) using measurements from all levels between 1000 m and 6000 m above ground. Potential temperature and q gradients in the free troposphere depend on synoptic conditions and can influence the diurnal development of T_a and VPD in the ABL in addition to surface inputs of sensible heat and water vapor fluxes (e.g. van Heerwaarden *et al* 2009). Atmospheric profile data were only used when the coefficient of determination between height and T_p (1000 m to 6000 m) was larger than 0.9, which was the case for 90% of all available days across all sites. Model simulations were run for each of the eight balloon sounding sites with peatland- and forest-specific land surface parameterizations (α , g_a , and g_s) and were forced with the ensemble of initial T_p and q and lapse rates derived from the sounding data at each site.

3. Results

Between February and September, median midday sensible heat fluxes were significantly ($p < 0.05$) higher for forests than for peatlands with absolute differences of about $120 W m^{-2}$ peaking at the end of winter in April (figure 2(a)). Between April and December, sensible heat flux differences decreased continuously. Median midday latent heat fluxes were higher for peatlands than for forests during the growing season between May and August reaching maximum differences of 60 to $70 W m^{-2}$ between May and July. Differences in energy partitioning were reflected in significantly higher midday Bowen ratios for forests than for peatlands between March and September (figure 2(b)). Bowen ratios of the forests peaked at 4.5 in late winter (March) and remained above 1 until June, indicating the greater partitioning of available energy to sensible heat. Between July

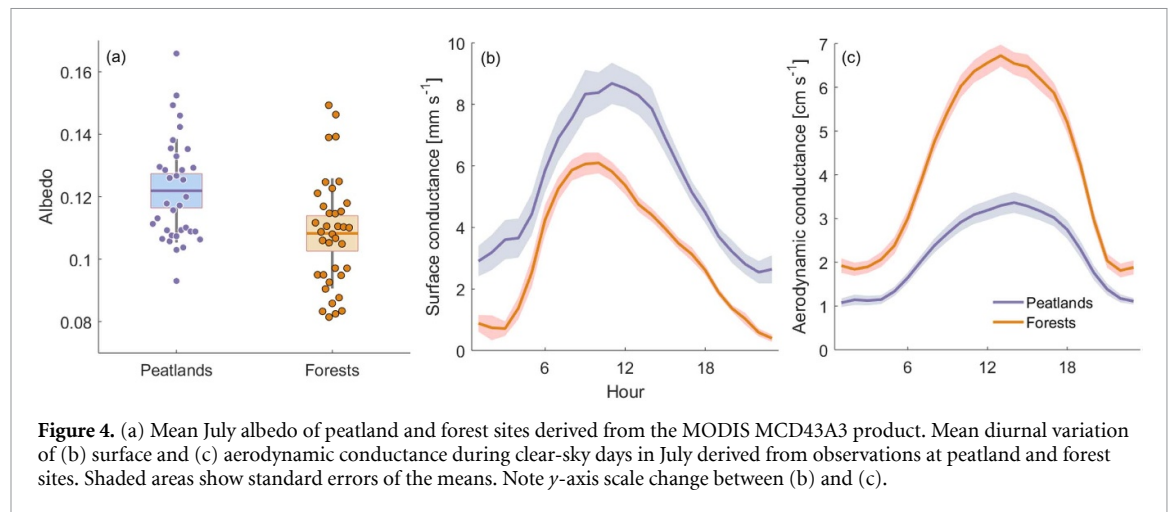


Figure 4. (a) Mean July albedo of peatland and forest sites derived from the MODIS MCD43A3 product. Mean diurnal variation of (b) surface and (c) aerodynamic conductance during clear-sky days in July derived from observations at peatland and forest sites. Shaded areas show standard errors of the means. Note y-axis scale change between (b) and (c).

and October, Bowen ratios of the forests were close to 1, indicating equal partitioning to sensible and latent heat. For peatlands, Bowen ratios remained below 1 throughout the year (i.e. latent heat exceeded sensible heat production). Bowen ratios of the peatlands peaked at about 0.8 in May and in October and reached a minimum of 0.5 in July.

In July, sensible and latent heat fluxes from forests and peatlands showed different diurnal magnitudes during clear-sky conditions with peak sensible heat fluxes from forests being on average 67% [$\pm 10\%$; $\pm \text{s.e.}$] higher than from peatlands (figure 3(a)) and peak latent heat fluxes from peatlands being 46% [$\pm 8\%$] higher than from forests (figure 3(b)). In contrast, peak net radiation for forests was only 8% [$\pm 4\%$] higher than that for peatlands (figure S4), highlighting the importance of ecosystem-specific differences in energy partitioning. Differences in energy partitioning led to mid-day Bowen ratios for forests (1.06 ± 0.33 ; $\pm \text{SD}$) being twice as high as for peatlands (0.50 ± 0.24 , figure 3(c)).

Ecosystem-specific land surface properties such as albedo and aerodynamic and surface conductances explain the observed energy flux differences. In July, forest albedo was on average slightly lower ($1 \pm 2\%$; $\pm \text{SD}$) than peatland albedo (figure 4(a)). Aerodynamically rougher forests were characterized by consistently larger g_a with maximum differences of 3 cm s^{-1} ($\sim 50\%$) in the early afternoon (figure 4(c)). In contrast, peatland g_s was consistently higher than forest g_s , with maximum differences of 3 mm s^{-1} ($\sim 30\%$) in the early afternoon (figure 4(b)).

The current potential peatland cooling effect on afternoon T_a (16 h local time) increased from 1.7°C to 2.5°C with decreasing latitude (from 68°N to 46°N) and with increasing SW_{in} (compared to forest afternoon T_a , figure 5(a)). This potential cooling effect is of similar magnitude to the projected ensemble-mean increase in daily near-surface maximum T_a in July in the boreal

biome for the Representative Concentration Pathway (RCP) 4.5 by eight Earth system models (interquartile range across boreal biome: 1.4 to 2.4°C (2091–2100 vs 2006–2015), Figure S5a, see table S3 for further details). Peatlands also contributed to more humid air with lower afternoon VPD (decrease of 0.4 to 0.7 kPa , figure 5(b)) compared to forests. The modelled decreases in VPD are in the same range as the projected increase in daily near-surface maximum VPD in July for the RCP8.5 (interquartile range across boreal biome: 0.4 to 0.8 kPa , figure S5b). Like the cooling effect, the moistening effect of peatlands increased from north to south. Modelled afternoon ABL heights over peatlands ($2122 \pm 84 \text{ m}$) were about 20% lower than over forests ($2655 \pm 96 \text{ m}$) (figure 5(c)).

4. Discussion

4.1. Boreal land cover impacts on regional climate

Land cover and land use change have been shown to alter local to regional climate, thereby modifying the impact of global climate change regionally (Diffenbaugh 2009, Luyssaert *et al* 2014, Huber *et al* 2014, Findell *et al* 2017, Zhang *et al* 2020). In the boreal biome, biophysical climate cooling due to fire disturbance, post-fire succession, deforestation, and shifts to deciduous forests has been reported (Bonan *et al* 1992, Chapin *et al* 2000, Randerson *et al* 2006, Lee *et al* 2011). These cooling effects were mainly driven by the higher albedo of non-forested and deciduous forest ecosystems during the snow-cover period compared to boreal conifer forests (e.g. Thomas and Rowntree 1992) and by higher albedo and lower Bowen ratios of deciduous forests during the growing season (e.g. Chapin *et al* 2000). Similar studies of biophysical climate impacts of boreal peatlands are rare and have often focussed on radiative (e.g. albedo) rather than non-radiative mechanisms (e.g. energy partitioning). For example, peatlands have been shown to have higher albedo than forests during the snowcover and growing season

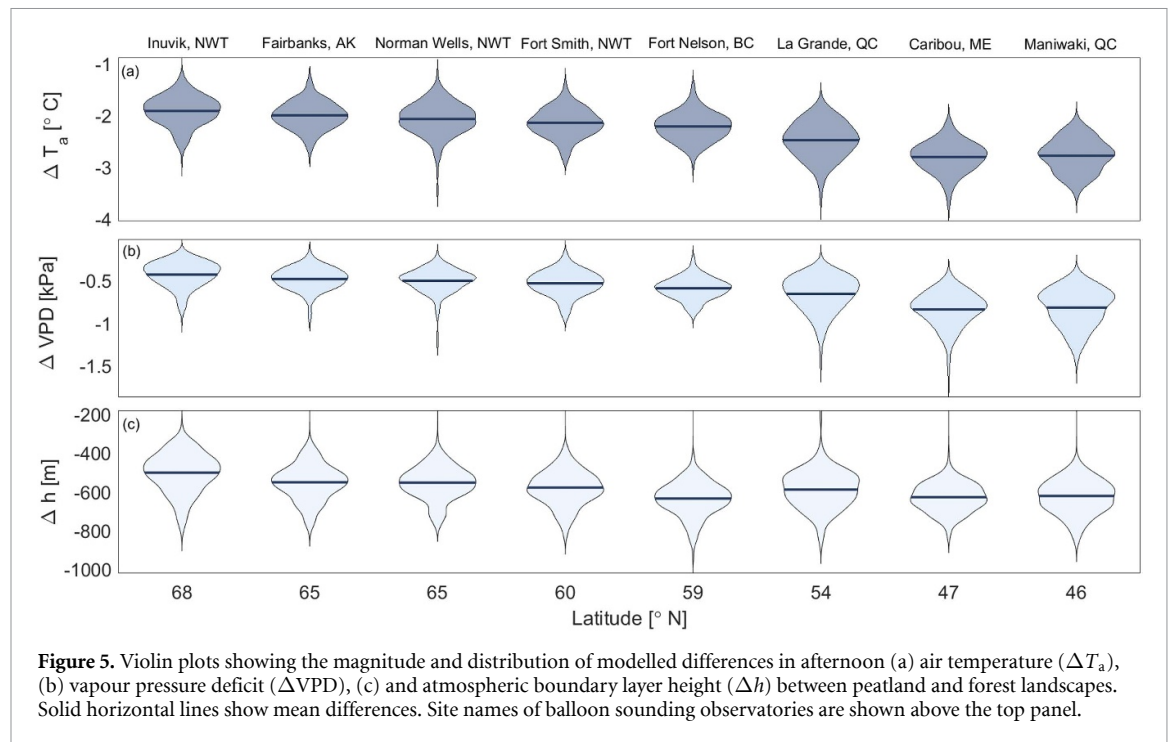


Figure 5. Violin plots showing the magnitude and distribution of modelled differences in afternoon (a) air temperature (ΔT_a), (b) vapour pressure deficit (ΔVPD), (c) and atmospheric boundary layer height (Δh) between peatland and forest landscapes. Solid horizontal lines show mean differences. Site names of balloon sounding observatories are shown above the top panel.

period with the strongest impacts on surface energy fluxes during the spring when incoming radiation is high (Chapin *et al* 2000, Vygodskaya *et al* 2007). Similarly, we show that peatland albedo is higher than forest albedo during the growing season across a range of boreal peatlands. However, both peatland and forest albedo can vary widely across the boreal biome due to factors such as vegetation composition (e.g. presence of highly reflective lichen; Petzold and Rencz (1975)), tree cover (Kuusinen *et al* 2016), and forest age (Kuusinen *et al* 2014).

Non-radiative effects on local and regional climates often exceed the radiative effects of albedo differences (Pielke *et al* 2002, Bright *et al* 2017). Similar to our study, Baldocchi *et al* (2000) and Helbig *et al* (2016b) have shown that boreal conifer forests in western North America produce higher sensible and lower latent heat fluxes than peatlands during the growing season resulting in deep ABLs over conifer forests (Pielke and Vidale 1995, Betts *et al* 2001). Here, we have demonstrated that the difference in ecosystem-specific energy partitioning of boreal peatlands and forests can cause regionally cooler growing season air temperatures and lower atmospheric water demand (i.e. lower VPD). In peatland-dominated boreal landscapes, biophysical climate impacts of peatlands can be of similar magnitude than projected increases in air temperature and atmospheric water demand (figure S5). However, in this study, we focus on peatland impacts on growing season clear-sky T_a and VPD, which likely represent the upper bound of climate impacts. Available energy flux is lower on cloudy days with lower SW_{in} when differences in energy partitioning likely have less impact on T_a and VPD (Betts

et al 2014). Accounting for cloud interactions in more complex ABL models in future studies would allow the quantification of climate impacts under a wider range of atmospheric conditions.

4.2. Forest disturbance impacts on regional climate in the boreal biome

Mature forests— as analyzed in this study—are the most prevalent forest type in the boreal biome. For example, Stinson *et al* (2011) estimate that about two thirds of Canada's managed forest lands has a stand age of 60 years or more. However, a substantial fraction of the boreal forest is affected by disturbances such as wildfires, insect outbreaks, and logging (e.g. Haeussler *et al* 2002, Seidl *et al* 2017). The early post-disturbance succession is often dominated by shrublands and deciduous-broadleaf dominated forests, while the late succession stages are usually dominated by deciduous and evergreen needleleaf forests (Amiro *et al* 2010). Albedo and energy partitioning can vary widely between these forest types with mature evergreen needleleaf forests usually featuring lower albedo and higher Bowen ratios (Chapin *et al* 2000, Randsen *et al* 2006, Amiro *et al* 2006). Thus, forest types other than mature evergreen needleleaf forests likely add to the biophysical cooling effect of peatlands as reported in this study.

Thawing permafrost represents another important disturbance mechanism in the boreal forest (e.g. Osterkamp *et al* 2000, Helbig *et al* 2016a, Carpino *et al* 2018). In ice-rich permafrost landscapes, thawing has been shown to lead to an expansion of treeless peatlands at the expense of boreal forests (Carpino *et al* 2018) exerting a regional climate cooling and

wetting effect (Helbig *et al* 2016b). Climate change is expected to further increase the occurrence of disturbance events in the boreal biome (Seidl *et al* 2017), leading to potentially even larger biophysical climate impacts.

4.3. Land cover impacts on the atmospheric water cycle and teleconnections

Differences in T_a and VPD between forests and peatlands cause lower lifting condensation levels in peatlands (i.e. height at which an air parcel becomes saturated) and lower Bowen ratios in peatlands lead to reduced ABL growth. Consequently, different peatland and forest impacts on cloud cover and precipitation patterns can be expected (e.g. Juang *et al* 2007). For example, decreasing Bowen ratios have been shown to influence cloud development (e.g. Gentine *et al* 2013) and convective precipitation dynamics (e.g. Gerken *et al* 2018). When a peatland parameterization was added to a regional weather prediction model, Yurova *et al* (2014) observed an increase in cloud cover for the peatland-dominated Western Siberian Lowlands. The biophysical climate impacts of peatlands may additionally contribute to the climate of remote areas through ecoclimatic teleconnections (i.e. propagation via atmospheric circulation; Swann *et al* 2012, Stark *et al* 2016). We therefore expect peatlands to not only affect T_a and VPD regionally, but also cloud cover and precipitation patterns (Yurova *et al* 2014) and climates across the continent (e.g. Stark *et al* 2016). However, only coupled Earth system model simulations are capable of quantifying these dynamic land-atmosphere feedbacks (e.g. Laguë *et al* 2019). Improved representation of peatlands in regional- and global-scale Earth system models is therefore necessary to fully understand the role of peatlands in regional and global climate systems (Helbig *et al* 2020).

4.4. Boreal landscapes as a mosaic of land cover types

Many boreal landscapes are characterized by small-scale patchiness (<1 km) in land cover types. Heterogeneous land cover leads to spatially variable albedo (e.g. Chen *et al* 2019) and surface energy fluxes (e.g. Starkenburg *et al* 2015). The heterogeneous structure of sensible and latent heat fluxes leads to the development of mesoscale atmospheric circulation (e.g. Mauder *et al* 2007, Eder *et al* 2015). As a result, air is mixed between forest, peatland, and lake patches leading to homogenization of daytime ABL depth over these landscapes. However, ABL growth has been shown to be mainly driven by large sensible heat input from conifer forests (Betts *et al* 2001). Within the ABL, the lateral advection of warm and dry air (e.g. from conifer forests) can enhance evapotranspiration from well-watered surfaces (such as peatlands) as shown by Baldocchi *et al* (2016) for rice paddies and

by Petrone *et al* (2007) for boreal riparian pond complexes. In this study, we assume spatial homogeneity in land cover types for our modelling experiments. Some regions such as the Hudson Bay Lowlands and the Western Siberian Lowlands are characterized by extensive peatland coverage. However, the absolute magnitude of the peatland cooling and moistening effect reported in this study is likely modified by the mosaic nature of most other boreal landscapes. How spatial heterogeneity affects land surface and ABL conditions depends mainly on the scale, patchiness, and spatial structure of individual land cover types (Mahrt 2000, Li and Wang 2019) and therefore will vary between boreal landscapes. The spatial heterogeneity and structure of land cover types therefore needs to be accounted for when quantifying the absolute biophysical climate mitigation impact of peatlands for different boreal landscapes. Such impacts can be quantified using large eddy simulations of land-atmosphere interactions (e.g. Albertson *et al* 2001, Huang and Margulis 2010).

4.5. Implications for land management

Our study highlights the need to include estimates for the biophysical climate mitigation potential of peatlands in cost-benefit assessments of peatland restoration. Recent studies have advocated for global-scale tree restoration including reforestation in the boreal biome since increased tree coverage can contribute to climate change mitigation through enhanced carbon sequestration (Bastin *et al* 2019). Boreal peatlands have been drained across the boreal biome for forestry (Laine *et al* 1995) and the related afforestation of boreal peatlands has indeed likely led to an increase in carbon sequestration (Minkinen *et al* 2002, Lohila *et al* 2010). However, our study shows that boreal conifer forests have also a biophysical warming effect on regional climate and can amplify atmospheric water stress, while boreal peatlands can exert a growing season climate cooling effect on afternoon air temperatures of up to 1.7 °C to 2.5 °C. In contrast, Gao *et al* (2014) report a slight cooling effect of peatland forestation in Finland using a regional climate model. They found differences in evapotranspiration to be the main driver of cooling during the growing season, but—unlike our study—their regional climate model simulated higher evapotranspiration rates over forested areas than over peatlands.

Peatland restoration in this context has been shown to have a substantial climate change mitigation potential (Leifeld and Menichetti 2018) since the long-term cooling effect of increased soil carbon sequestration exceeds the short-term warming impact of simultaneous increases in methane emissions (Frolking and Roulet 2007, Günther *et al* 2020). Additionally, peatland restoration can contribute to other ecosystem services such as increasing biodiversity, improving water quality, and supporting flood protection (Zedler and Kercher 2005).

However, it is unclear how peatland restoration can modify regional climates. While peatland restoration has been shown to have the potential to cool land surface temperature compared to surrounding agricultural land (Hemes *et al* 2018, Worrall *et al* 2019), biophysical impacts of land cover changes on surface and air temperature can differ substantially (Winckler *et al* 2019, Novick and Katul 2020).

Our study focuses on biophysical climate impacts of boreal peatlands. However, drainage has degraded larger peatland areas in the temperate than in the boreal zone. Consequently, many restoration efforts focus on temperate peatlands (Günther *et al* 2020). Here, we have shown that the biophysical climate cooling and humidifying effect is more pronounced at the southern limit of the boreal biome. Thus, we also expect a substantial biophysical climate mitigation potential for temperate peatlands. However, their climate impacts likely differ from boreal peatlands in many cases since temperate peatlands have often been converted into grasslands or other agricultural land (Günther *et al* 2020). In this case, climate cooling effects would differ compared to effects resulting from forest-to-peatland conversion. Additionally, large-scale temperate peatland restoration may be less feasible than large-scale boreal peatland conservation due to widespread existing anthropogenic land use in the temperate zone (e.g. Moore 2002, Andersen *et al* 2017, Günther *et al* 2020). With a warmer and drier climate, climatic conditions suitable to sustain peatland ecosystems are likely to become rarer in the temperate zone and at the southern limit of the boreal biome (e.g. Hoppo *et al* 2020, Helbig *et al* 2020) and could jeopardise any peatland restoration efforts. Loss of peatland area could then lead to additional regional warming and drying through biophysical climate impacts. Preventing or minimising such positive feedback requires efforts to limit anthropogenic influences on climate change.

In addition to drainage of peatlands for forestry, peatlands have been degraded for horticultural purposes and for oil and gas extraction (Chimner *et al* 2017). Compared to degraded peatlands, natural peatland evapotranspiration has been found to be higher (Mccarter and Price 2013) and an increase in evapotranspiration following rewetting of a degraded peatland was reported by Ketcheson and Price (2011). Thus, similar to restoration of peatlands that were drained for forestry, the restoration of peatlands after peat extraction or mining activities may have a biophysical climate mitigation potential.

A better understanding of biophysical controls of peatlands on climate will help quantify peatland impacts on present and future climates in the boreal biome, and can support land management policies aiming at mitigating climate change. This policy input is especially relevant given the urgent need to restore the over 300 000 km² of boreal and temperate peatlands having been mined or drained for agriculture

and forestry (Günther *et al* 2020) and to conserve and protect pristine peatlands.

Acknowledgments

We thank the two anonymous reviewers for their feedback on our work, which has substantially improved this article.

This work is part of the Boreal Water Futures project and supported through the Global Water Futures research program. We thank all the EC flux tower teams for sharing their data. We are grateful to Myroslava Khomik, Adam Green, Inke Forbrich, Eric Kessel, Gordon Drewitt, and Pasi Kolari for helping with data preparation and to Inke Forbrich on feedback on an earlier version of the manuscript.

I M acknowledges funding from ICOS-FINLAND (Grant 281255), Finnish Center of Excellence (Grant 307331), and EU Horizon-2020 RINGO project (Grant 730944). A P acknowledges funding through the research project # 18-45-243003 (RFBR and Government of Krasnoyarsk Territory, Krasnoyarsk Regional Fund of Science) and support for flux tower sites RU-ZOP and RU-ZOB through the Max Planck Society. A D and J T acknowledges funding from US National Science foundation #DEB-1440297 and DOE Ameriflux Network Management Project award to ChEAS core site cluster. T A B, A G B, and R J acknowledge support received through grants from the Fluxnet Canada ResearchNetwork (2002–2007; NSERC, CFCAS, and BIOCAP) and the Canadian Carbon Program (2008–2012; CFCAS) and by an NSERC (Climate Change and Atmospheric Research) Grant to the Changing Cold Regions Network (CCRN; 2012–2016) and an NSERC Discovery Grant. H I and M U acknowledge support by the Arctic Challenge for Sustainability II (ArCS II) project (JPMXD1420318865). J K and A V acknowledge funding by RFBR project number 19-04-01234-a. B A acknowledges funding through NASA, NSERC, BIOCAP Canada, the Canadian Foundation for Climate and Atmospheric Sciences, and the Canadian Foundation for Innovation for flux measurements at CA-MAN and through the Canadian Forest Service, the Natural Sciences and Engineering Research Council of Canada (NSERC), the FLUXNET-Canada Network (NSERC, the Canadian Foundation for Climate and Atmospheric Sciences (CFCAS), and BIOCAP Canada), the Canadian Carbon Program (CFCAS), Parks Canada, and the Program of Energy Research and Development (PERD). O S acknowledges funding by the Canada Research Chairs, Canada Foundation for Innovation Leaders Opportunity Fund, and Natural Sciences and Engineering Research Council Discovery Grant Programs. L B F acknowledges funding from the Natural Sciences and Engineering Research Council of Canada (NSERC), the FLUXNET-Canada Network (NSERC,

the Canadian Foundation for Climate and Atmospheric Sciences (CFCAS), and BIOCAP Canada), and the Canadian Carbon Program (CFCAS). M B N, M O L, M P, and J C gratefully acknowledge funding from the Swedish research infrastructures SITES and ICOS Sweden and research grants from Kempe Foundations, (#SMK-1743); VR (#2018-03966) and Formas, (#2016-01289) and M P gratefully acknowledges funding from Knut and Alice Wallenberg Foundation (#2015.0047).

M W acknowledge funding by the German Research Foundation (Grant Wi 2680/2-1) and the European Union (Grant 36993). B R K R and L K acknowledge support by the Cluster of Excellence 'CliSAP' (EXC177) of the University of Hamburg, funded by the German Research Foundation. H I acknowledges JAMSTEC and IARC/UAF collaboration study (JICS) and Arctic Challenge for Sustainability Project (ArCS). E H acknowledges the support of the FLUXNET-Canada Network, the Canadian Carbon Program, and Ontario Ministry of the Environment, Conservation and Parks. E L acknowledges funding by RFBR and Government of the Khanty-Mansi Autonomous Okrug — Yugra project # 18-44-860017 and grant of the Yugra State University (13-01-20/39). M G and P T acknowledge NSERC funding (RDCPJ514218). M A, M K, A L. and J P T acknowledge the support by the Ministry of Transport and Communication through ICOS-Finland, Academy of Finland (grants 296888 and 308511), and Maj and Tor Nessling Foundation. T M acknowledge funding by Yakutian Scientific Center of Siberian Branch of Russian Academy of Sciences (Grant FWRS-2020-0012).

Code availability

All MATLAB code used in this study is available through the corresponding author's GitHub repository (<https://github.com/manuelhelbig/PeatlandCooling>) and is available from the corresponding author upon request. The software used to generate all results is MATLAB 2016a.

Data availability statement

The data that support the findings of this study are available upon reasonable request from the authors.

ORCID iDs

Manuel Helbig  <https://orcid.org/0000-0003-1996-8639>

James M Waddington  <https://orcid.org/0000-0002-0317-7894>

Pavel Alekseychik  <https://orcid.org/0000-0002-4081-3917>

Brian Amiro  <https://orcid.org/0000-0002-9969-0050>

Mika Aurela  <https://orcid.org/0000-0002-4046-7225>

Alan G Barr  <https://orcid.org/0000-0003-2717-218X>

Sean K Carey  <https://orcid.org/0000-0002-3316-228X>

Jiquan Chen  <https://orcid.org/0000-0003-0761-9458>

Jinshu Chi  <https://orcid.org/0000-0001-5688-8895>

Ankur R Desai  <https://orcid.org/0000-0002-5226-6041>

Allison Dunn  <https://orcid.org/0000-0003-1960-6718>

Eugenie S Euskirchen  <https://orcid.org/0000-0002-0848-4295>

Lawrence B Flanagan  <https://orcid.org/0000-0003-1748-0306>

Thomas Friborg  <https://orcid.org/0000-0001-5633-6097>

Achim Grelle  <https://orcid.org/0000-0003-3468-9419>


Silvie Harder  <https://orcid.org/0000-0002-9350-9927>

Michal Heliasz  <https://orcid.org/0000-0003-2635-9604>

Elyn R Humphreys  <https://orcid.org/0000-0002-5397-2802>

Hiroki Ikawa  <https://orcid.org/0000-0002-4984-8067>

Pierre-Erik Isabelle  <https://orcid.org/0000-0002-2819-1377>

Hiroki Iwata  <https://orcid.org/0000-0002-8962-8982>

Rachhpal Jassal  <https://orcid.org/0000-0002-6727-5215>

Mika Korkiakoski  <https://orcid.org/0000-0001-6875-9978>

Juliya Kurbatova  <https://orcid.org/0000-0003-4452-7376>

Lars Kutzbach  <https://orcid.org/0000-0003-2631-2742>

Elena Lapshina  <https://orcid.org/0000-0001-5571-7787>

Anders Lindroth  <https://orcid.org/0000-0002-7669-784X>

Annalea Lohila  <https://orcid.org/0000-0003-3541-672X>

Ivan Mammarella  <https://orcid.org/0000-0002-8516-3356>

Philip Marsh  <https://orcid.org/0000-0002-3618-6893>

Paul A Moore  <https://orcid.org/0000-0003-1924-1528>

Daniel F Nadeau  <https://orcid.org/0000-0002-4006-2623>

Erin M Nicholls  <https://orcid.org/0000-0002-8102-7285>

Mats B Nilsson  <https://orcid.org/0000-0003-3765-6399>

Matthias Peichl  <https://orcid.org/0000-0002-9940-5846>

Anatoly Prokushkin  <https://orcid.org/0000-0001-8721-2142>

William L Quinton  <https://orcid.org/0000-0001-5707-4519>

Nigel Roulet  <https://orcid.org/0000-0001-9571-1929>

Benjamin R K Runkle  <https://orcid.org/0000-0002-2583-1199>

Oliver Sonnentag  <https://orcid.org/0000-0001-9333-9721>

Ian B Strachan  <https://orcid.org/0000-0001-6457-5530>

Pierre Taillardat  <https://orcid.org/0000-0003-0195-3690>

Juha-Pekka Tuovinen  <https://orcid.org/0000-0001-7857-036X>

Jessica Turner  <https://orcid.org/0000-0003-1532-4174>

Masahito Ueyama  <https://orcid.org/0000-0002-4000-4888>

Andrej Varlagin  <https://orcid.org/0000-0002-2549-5236>

Timo Vesala  <https://orcid.org/0000-0002-4852-7464>

Martin Wilmking  <https://orcid.org/0000-0003-4964-2402>

References

- Ackerly D D, Loarie S R, Cornwell W K, Weiss S B, Hamilton H, Branciforte R and Kraft N J B 2010 The geography of climate change: implications for conservation biogeography *Divers. Distrib.* **16** 476–87
- Albertson J D, Kustas W P and Scanlon T M 2001 Large-eddy simulation over heterogeneous terrain with remotely sensed land surface conditions *Water Resour. Res.* **37** 1939–53
- Alekseychik P et al 2018 Surface energy exchange in pristine and managed boreal peatlands *Mires Peat* **21** 14
- Allen R, Walter I, Elliott R, Howell T, Itenfisu D, Jensen M and Snyder R 2005 *The ASCE standardized reference evapotranspiration equation* (Reston, VA: American Society of Civil Engineers) www.ars.usda.gov/research/publications/publication/?seqNo115=199130
- Amiro B D et al 2010 Ecosystem carbon dioxide fluxes after disturbance in forests of North America *J. Geophys. Res.* **115** G00K02
- Amiro B D et al 2006 The effect of post-fire stand age on the boreal forest energy balance *Agric. For. Meteorol.* **140** 41–50
- Andersen R, Farrell C, Graf M, Muller F, Calvar E, Frankard P, Caporn S and Anderson P 2017 An overview of the progress and challenges of peatland restoration in Western Europe *Restor. Ecol.* **25** 271–82
- Anderson R G et al 2011 Biophysical considerations in forestry for climate protection *Front. Ecol. Environ.* **9** 174–82
- Bagley J E, Desai A R, West P C and Foley J A 2011 A simple, minimal parameter model for predicting the influence of changing land cover on the land–atmosphere system *Earth Interact.* **15** 1–32
- Baldocchi D, Kelliher F M, Black T A and Jarvis P 2000 Climate and vegetation controls on boreal zone energy exchange *Global Change Biol.* **6** 69–83
- Baldocchi D, Knox S, Dronova I, Verfaillie J, Oikawa P, Sturtevant C, Matthes J H and Detto M 2016 The impact of expanding flooded land area on the annual evaporation of rice *Agric. For. Meteorol.* **223** 181–93
- Baldocchi D and Ma S 2013 How will land use affect air temperature in the surface boundary layer? Lessons learned from a comparative study on the energy balance of an oak savanna and annual grassland in California, USA *Tellus B* **65** 19994
- Bastin J-F, Finegold Y, Garcia C, Mollicone D, Rezende M, Routh D, Zohner C M and Crowther T W 2019 The global tree restoration potential *Science* **365** 76–79
- Betts A K, Ball J H and Mccaughey J H 2001 Near-surface climate in the boreal forest *J. Geophys. Res.* **106** 33,529–33,541
- Betts A K, Desjardins R, Worth D and Beckage B 2014 Climate coupling between temperature, humidity, precipitation, and cloud cover over the Canadian Prairies *J. Geophys. Res.* **119** 13,305–13,326
- Betts R A 2000 Offset of the potential carbon sink from boreal forestation by decreases in surface albedo *Nature* **408** 187–90
- Bonan G B 2008 Forests and Climate Change: forcings, feedbacks, and the climate benefits of forests *Science* **320** 1444–9
- Bonan G B, Pollard D and Thompson S L 1992 Effects of boreal forest vegetation on global climate *Clim. Nat.* **359** 716–8
- Bright R M, Davin E, O'Halloran T, Pongratz J, Zhao K and Cescatti A 2017 Local temperature response to land cover and management change driven by non-radiative processes *Nat. Clim. Change* **7** 296–302
- Brutsaert W 1975 On a derivable formula for long-wave radiation from clear skies *Water Resour. Res.* **11** 742–4
- Carpino O A, Berg A A, Quinton W L and Adams J R 2018 Climate change and permafrost thaw-induced boreal forest loss in northwestern Canada *Environ. Res. Lett.* **13** 084018
- Chapin F S et al 2000 Arctic and boreal ecosystems of western North America as components of the climate system *Global Change Biol.* **6** 211–23
- Chapman S et al 2003 Exploitation of northern peatlands and biodiversity maintenance: a conflict between economy and ecology *Front. Ecol. Environ.* **1** 525–32
- Chen J, Sciusco P, Ouyang Z, Zhang R, Henebry G M, John R and Roy David P 2019 Linear downscaling from MODIS to Landsat: connecting landscape composition with ecosystem functions *Landscape Ecol.* **34** 2917–34
- Chimner R A, Cooper D J, Wurster F C and Rochefort L 2017 An overview of peatland restoration in North America: where are we after 25 years? *Restor. Ecol.* **25** 283–92
- Combe M, de Arellano J V-G, Ouwersloot H G and Peters W 2016 Plant water-stress parameterization determines the strength of land–atmosphere coupling *Agric. For. Meteorol.* **217** 61–73
- De Frenne P et al 2013 Microclimate moderates plant responses to macroclimate warming *Proc. Natl Acad. Sci.* **110** 18561–5
- Diffenbaugh N S 2009 Influence of modern land cover on the climate of the United States *Clim. Dyn.* **33** 945
- Eder F, De Roo F, Rotenberg E, Yakir D, Schmid H P and Mauder M 2015 Secondary circulations at a solitary forest surrounded by semi-arid shrubland and their impact on eddy-covariance measurements *Agric. For. Meteorol.* **211–212** 115–27
- Esseen P-A, Ehnström B, Ericson L and Sjöberg K 1997 Boreal Forests *Ecol. Bull.* **16**–47
- Findell K L, Berg A, Gentile P, Krasting J P, Lintner B R, Malyshev S, Santanello J A and Shevliakova E 2017 The impact of anthropogenic land use and land cover change on regional climate extremes *Nat. Commun.* **8** 1–10
- Friedlingstein P et al 2019 Global Carbon Budget 2019 *Earth Syst. Sci. Data* **11** 1783–838
- Frolking S and Roulet N T 2007 Holocene radiative forcing impact of northern peatland carbon accumulation and methane emissions *Global Change Biol.* **13** 1079–88
- Gao Y, Markkanen T, Backman L, Henttonen H M, Pietikäinen J-P, Mäkelä H M and Laaksonen A 2014 Biogeophysical impacts of peatland forestation on regional climate changes in Finland *Biogeosciences* **11** 7251–67

- Gauthier S, Bernier P, Kuuluvainen T, Shvidenko A Z and Schepaschenko D G 2015 Boreal forest health and global change *Science* **349** 819–22
- Gentine P, Ferguson C R and Holtslag A A M 2013 Diagnosing evaporative fraction over land from boundary-layer clouds *J. Geophys. Res. Atmos.* **118** 8185–96
- Gerken T, Bromley G T and Stoy P C 2018 Surface moistening trends in the Northern North American great plains increase the likelihood of convective initiation *J. Hydrometeorol* **19** 227–44
- Günther A, Barthelmes A, Huth V, Joosten H, Jurasinski G, Koebisch F and Couwenberg J 2020 Prompt rewetting of drained peatlands reduces climate warming despite methane emissions *Nat. Commun.* **11** 1644
- Haeussler S, Bedford L, Leduc A, Bergeron Y and Kranabetter J 2002 Silvicultural disturbance severity and plant communities of the southern Canadian boreal forest *Silva Fenn.* **36** 307–27
- Helbig M et al 2020 Increasing contribution of peatlands to boreal evapotranspiration in warming climate *Nat. Clim. Change* **10** 555–60
- Helbig M, Pappas C and Sonnentag O 2016a Permafrost thaw and wildfire: equally important drivers of boreal tree cover changes in the Taiga Plains *Geophys. Res. Lett.* **43** 1598–606
- Helbig M, Wischniewski K, Kljun N, Chasmer L E, Quinton W L, Detto M and Sonnentag O 2016b Regional atmospheric cooling and wetting effect of permafrost thaw-induced boreal forest loss *Global Change Biol.* **22** 4048–66
- Hemes K S, Eichelmann E, Chamberlain S D, Knox S H, Oikawa P Y, Sturtevant C, Verfaillie J, Szutu D and Baldocchi D D 2018 A Unique combination of aerodynamic and surface properties contribute to surface cooling in restored wetlands of the Sacramento-San Joaquin Delta, California *J. Geophys. Res.* **123** 2072–90
- Hopple A M, Wilson R M, Kolton M, Zalman C A, Chanton J P, Kostka J, Hanson P J, Keller J K and Bridgman S D 2020 Massive peatland carbon banks vulnerable to rising temperatures *Nat. Commun.* **11** 2373
- Huang H-Y and Margulis S A 2010 Evaluation of a fully coupled large-eddy simulation–land surface model and its diagnosis of land-atmosphere feedbacks *Water Resour. Res.* **46** W06512
- Huber D, Mechum D and Brunsell N 2014 The effects of Great Plains irrigation on the surface energy balance, regional circulation, and precipitation *Climate* **2** 103–28
- Humphreys E R, Lafleur P M, Flanagan L B, Hedstrom N, Syed K H, Glenn A J and Granger R 2006 Summer carbon dioxide and water vapor fluxes across a range of northern peatlands *J. Geophys. Res.* **111** G04011
- Jarvis P G 1976 The interpretation of the variations in leaf water potential and stomatal conductance found in canopies in the field *Philos. Trans. R. Soc. B* **273** 593–610
- Juang J-Y, Katul G G, Porporato A, Stoy P C, Siqueira M S, Detto M, Kim H-S and Oren R 2007 Eco-hydrological controls on summertime convective rainfall triggers *Global Change Biol.* **13** 887–96
- Ketcheson S J and Price J S 2011 The impact of peatland restoration on the site hydrology of an abandoned block-cut bog *Wetlands* **31** 1263–74
- Kuusinen N, Stenberg P, Korhonen L, Rautiainen M and Tomppo E 2016 Structural factors driving boreal forest albedo in Finland *Remote Sens. Environ.* **175** 43–51
- Kuusinen N, Tomppo E, Shuai Y and Berninger F 2014 Effects of forest age on albedo in boreal forests estimated from MODIS and Landsat albedo retrievals *Remote Sens. Environ.* **145** 145–53
- Lafleur P M 2008 Connecting atmosphere and wetland: energy and water vapour exchange *Geography. Compass* **2** 1027–57
- Lafleur P M, Hember R A, Admiral S W and Roulet N T 2005 Annual and seasonal variability in evapotranspiration and water table at a shrub-covered bog in southern Ontario (Canada) *Hydrol. Process.* **19** 3533–50
- Laguë M M, Bonan G B and Swann A L S 2019 Separating the impact of individual land surface properties on the terrestrial surface energy budget in both the coupled and uncoupled land–atmosphere system *J. Climate* **32** 5725–44
- Laine J, Vasander H and Sallantausta T 1995 Ecological effects of peatland drainage for forestry *Environ. Rev.* **3** 286–303
- Lee X et al 2011 Observed increase in local cooling effect of deforestation at higher latitudes *Nature* **479** 384–7
- Leifeld J and Menichetti L 2018 The underappreciated potential of peatlands in global climate change mitigation strategies *Nat. Commun.* **9** 1071
- Li D and Wang L 2019 Sensitivity of surface temperature to land use and land cover change-induced biophysical changes: the scale issue *Geophys. Res. Lett.* **46** 9678–89
- Lohila A, Minkinen K, Laine J, Savolainen I, Tuovinen J-P, Korhonen L, Laurila T, Tietäväinen H and Laaksonen A 2010 Forestation of boreal peatlands: impacts of changing albedo and greenhouse gas fluxes on radiative forcing *J. Geophys. Res.* **115** G04011
- Loisel J et al 2014 A database and synthesis of northern peatland soil properties and Holocene carbon and nitrogen accumulation *Holocene* **24** 1028–42
- Luyssaert S et al 2014 Land management and land-cover change have impacts of similar magnitude on surface temperature *Nat. Clim. Change* **4** 389–93
- Mahrt L 2000 Surface heterogeneity and vertical structure of the boundary layer *Boundary Layer Meteorol.* **96** 33–62
- Mauder M, Desjardins R L and Macpherson I 2007 Scale analysis of airborne flux measurements over heterogeneous terrain in a boreal ecosystem *J. Geophys. Res.* **112** D13112
- Mccarter C P R and Price J S 2013 The hydrology of the Bois-des-Bel bog peatland restoration: 10 years post-restoration *Ecol. Eng.* **55** 73–81
- Minkinen K, Korhonen R, Savolainen I and Laine J 2002 Carbon balance and radiative forcing of Finnish peatlands 1900–2100 – the impact of forestry drainage *Global Change Biol.* **8** 785–99
- Monteith J L 1965 Evaporation and environment *Symp. Soc. Exp. Biol.* **19** 205–34
- Moore P A, Pypker T G and Waddington J M 2013 Effect of long-term water table manipulation on peatland evapotranspiration *Agric. For. Meteorol.* **178–179** 106–19
- Moore P D 2002 The future of cool temperate bogs *Environ. Conserv.* **29** 3–20
- Mäkelä A, Kolari P, Karimäki J, Nikinmaa E, Perämäki M and Hari P 2006 Modelling five years of weather-driven variation of GPP in a boreal forest *Agric. For. Meteorol.* **139** 382–98
- Novick K A and Katul G G 2020 The duality of reforestation impacts on surface and air temperature *J. Geophys. Res.* **125** e2019JG005543
- Novick K A et al 2016 The increasing importance of atmospheric demand for ecosystem water and carbon fluxes *Nat. Clim. Change* **6** 1023–7
- Olson D M et al 2001 Terrestrial ecoregions of the world: a new map of life on Earth *BioScience* **51** 933
- Osterkamp T E, Viereck L, Shur Y, Jorgenson M T, Racine C, Doyle A and Boone R D 2000 Observations of thermokarst and its impact on boreal forests in Alaska, U.S.A. *Arct. Antarct. Alp. Res.* **32** 303–15
- Paw U K T 1987 Mathematical analysis of the operative temperature and energy budget *J. Therm. Biol.* **12** 227–33
- Petrone R M, Silins U and Devito K J 2007 Dynamics of evapotranspiration from a riparian pond complex in the Western Boreal Forest, Alberta, Canada *Hydrol. Process.* **21** 1391–401
- Petzold D E and Rencz A N 1975 The albedo of selected subarctic surfaces *Arct. Alp. Res.* **7** 393
- Pielke R A, Marland G, Betts R A, Chase T N, Eastman J L, Niles J O, Niyogi D D S and Running S W 2002 The influence of land-use change and landscape dynamics on the climate system: relevance to climate-change policy beyond

- the radiative effect of greenhouse gases *Phil. Trans. R. Soc. A* **360** 1705–19
- Pielke R A and Vidale P L 1995 The boreal forest and the polar front *J. Geophys. Res.* **100** 25755–8
- Poulter B, Ciais P, Hodson E, Lischke H, Maignan F, Plummer S and Zimmermann N E 2011 Plant functional type mapping for earth system models *Geosci. Model Dev.* **4** 993–1010
- Randerson J T *et al* 2006 The impact of boreal forest fire on climate warming *Science* **314** 1130–2
- Raupach M R 1995 Vegetation-atmosphere interaction and surface conductance at leaf, canopy and regional scales *Agric. For. Meteorol.* **73** 151–79
- Rooney R C, Bayley S E and Schindler D W 2012 Oil sands mining and reclamation cause massive loss of peatland and stored carbon *PNAS* **109** 4933–7
- Schaaf C and Wang Z 2015 MCD43A3 MODIS/Terra+Aqua BRDF/Albedo Daily L3 Global - 500m V006 [Data set]
- Schulze E-D, Kelliher F M, Körner C, Lloyd J and Leuning R 1994 Relationships among maximum stomatal conductance, ecosystem surface conductance, carbon assimilation rate, and plant nitrogen nutrition: A Global Ecology Scaling Exercise *Annu. Rev. Ecol. Syst.* **25** 629–62
- Schulze E-D, Leuning R and Kelliher F M 1995 Environmental regulation of surface conductance for evaporation from vegetation *Vegetatio* **121** 79–87
- Seidl R *et al* 2017 Forest disturbances under climate change *Nat. Clim. Change* **7** 395–402
- Stark S C *et al* 2016 Toward accounting for ecoclimate teleconnections: intra- and inter-continental consequences of altered energy balance after vegetation change *Landscape Ecol.* **31** 181–94
- Starkenburg D, Fochesatto G J, Cristóbal J, Prakash A, Gens R, Alfieri J G, Nagano H, Harazono Y, Iwata H and Kane D L 2015 Temperature regimes and turbulent heat fluxes across a heterogeneous canopy in an Alaskan boreal forest *J. Geophys. Res.* **120** 1348–60
- Stinson G *et al* 2011 An inventory-based analysis of Canada's managed forest carbon dynamics, 1990 to 2008 *Global Change Biol.* **17** 2227–44
- Swann A L S, Fung I Y and Chiang J C H 2012 Mid-latitude afforestation shifts general circulation and tropical precipitation *PNAS* **109** 712–6
- Swann A L, Fung I Y, Levis S, Bonan G B and Doney S C 2010 Changes in Arctic vegetation amplify high-latitude warming through the greenhouse effect *PNAS* **107** 1295–300
- Thomas G and Rowntree P R 1992 The boreal forests and climate *Q. J. R. Meteorol. Soc.* **118** 469–97
- Trugman A T, Medvigy D, Anderegg W R L and Pacala S W 2018 Differential declines in Alaskan boreal forest vitality related to climate and competition *Global Change Biol.* **24** 1097–107
- Turunen J 2008 Development of Finnish peatland area and carbon storage *Boreal Environ. Res.* **13** 319–34
- Verma S B 1989 Aerodynamic resistances to transfers of heat, mass and momentum *Estimation Areal Evapotranspiration* 177IAHS Publications vol (Vancouver, B.C.) 13–20
- Vilà-Guerau de Arellano J, van Heerwaarden C C, van Stratum J H B and van den Dries K 2015 *Atmospheric Boundary Layer: Integrating Air Chemistry and Land Interactions* (Cambridge: Cambridge University Press)
- Vygodskaya N N, Groisman P Y, Tchebakova N M, Kurbatova J A, Panforyov O, Parfenova E I and Sogachev A F 2007 Ecosystems and climate interactions in the boreal zone of northern Eurasia *Environ. Res. Lett.* **2** 045033
- Way D A, Crawley C and Sage R F 2013 A hot and dry future: warming effects on boreal tree drought tolerance *Tree Physiol.* **33** 1003–5
- Will R E, Wilson S M, Zou C B and Hennessey T C 2013 Increased vapor pressure deficit due to higher temperature leads to greater transpiration and faster mortality during drought for tree seedlings common to the forest-grassland ecotone *New Phytol.* **200** 366–74
- Winckler J, Reick C H, Luyssaert S, Cescatti A, Stoy P C, Lejeune Q, Raddatz T, Chlond A, Heidkamp M and Pongratz J 2019 Different response of surface temperature and air temperature to deforestation in climate models *Earth Syst. Dynam.* **10** 473–84
- Worrall F, Boothroyd I M, Gardner R L, Howden N J K, Burt T P, Smith R, Mitchell L, Kohler T and Gregg R 2019 The impact of peatland restoration on local climate: restoration of a cool humid island *J. Geophys. Res.* **124** 1696–713
- Wouters H, Petrova I Y, van Heerwaarden C C, Vilà-Guerau de Arellano J, Teuling A J, Meulenbergh V, Santanello J A and Miralles D G 2019 Atmospheric boundary layer dynamics from balloon soundings worldwide: CLASS4GL v1.0 *Geosci. Model Dev.* **12** 2139–53
- Xu J, Morris P J, Liu J and Holden J 2018 PEATMAP: refining estimates of global peatland distribution based on a meta-analysis *CATENA* **160** 134–40
- Yurova A, Tolstykh M, Nilsson M and Sirin A 2014 Parameterization of mires in a numerical weather prediction model *Water Resour. Res.* **50** 8982–96
- Zedler J B and Kercher S 2005 WETLAND RESOURCES: status, trends, ecosystem services, and restorability *Annu. Rev. Environ. Resour.* **30** 39–74
- Zhang Q *et al* 2020 Reforestation and surface cooling in temperate zones: mechanisms and implications *Global Change Biol.* **26** 3384–3401
- van Heerwaarden C C, Vilà-Guerau de Arellano J, Gounou A, Guichard F and Couvreux F 2010 Understanding the daily cycle of evapotranspiration: a method to quantify the influence of forcings and feedbacks *J. Hydrometeorol.* **11** 1405–22
- van Heerwaarden C C, Vilà-Guerau de Arellano J, Moene A F and Holtslag A A M 2009 Interactions between dry-air entrainment, surface evaporation and convective boundary-layer development *Q.J.R. Meteorol. Soc.* **135** 1277–91